Electronic supplementary information

Thermal relaxation and collective dynamics in interacting aerosol-generated hexagonal $NiFe_2O_4$ nanoparticles

D. Ortega,[a,b*] M. V. Kuznetsov,[c] Yu. G. Morozov,[d] O. V. Belousova[d] and I. P. Parkin[e]

[a] Instituto Madrileño de Estudios Avanzados en Nanociencia (IMDEA-Nanociencia), Cantoblanco 28049, Madrid, Spain
[b] Institute of Biomedical Engineering, University College London, WC1E 6BT London, UK
[c] N. P. Ogarev Mordovian State University, Saransk, Republic of Mordovia, 430005 Russia
[d] Institute of Structural Macrokinetics and Materials Science, Chernogolovka, Moscow Region, 142432, Russia
[e] Department of Chemistry, Materials Chemistry Centre, University College London, 20 Gordon Street, London, UK, WC1H 0AJ

*E-mail address: d.ponce@ucl.ac.uk

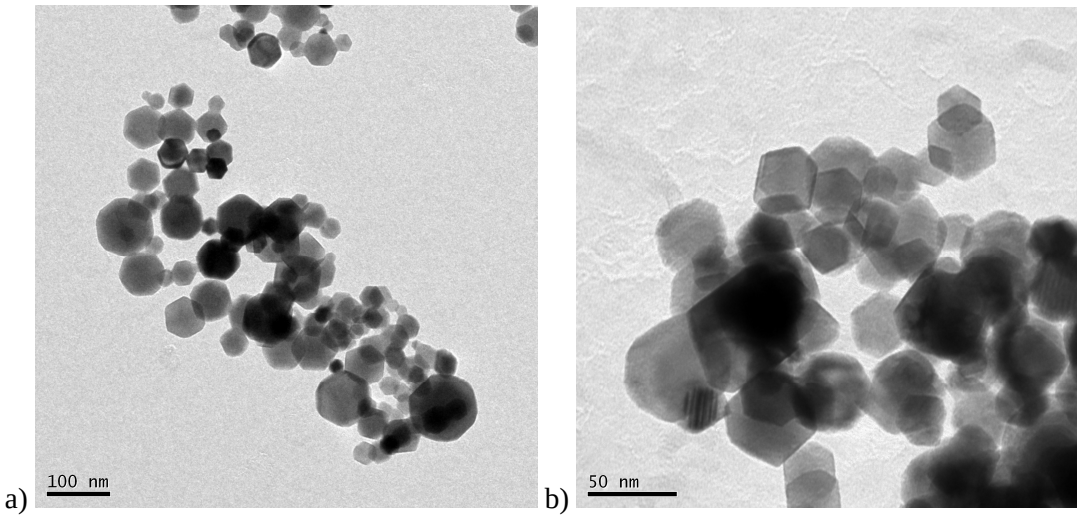

Fig. S1 Bright TEM images of samples M10 (a) and M13 (b).

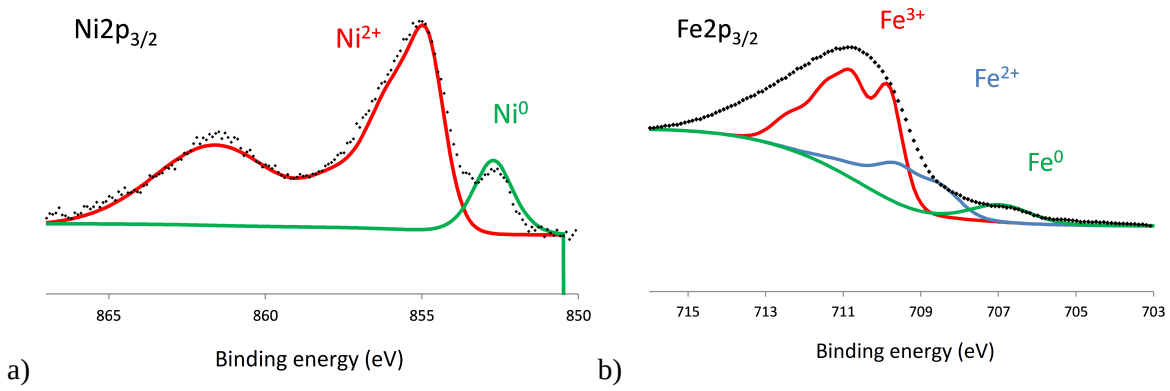

Fig. S2. Room temperature XPS spectra from sample M19 showing Ni (a) and Fe (b) contributions.

Table S2. Summary of the main magnetic properties for selected samples prepared under zero field. Synthesis conditions can be found in Table 1.

Sample ID	σ_s, A m^{2}kg^{-1}	σ_r, A m^{2}kg^{-1}	$\mu_0 H_c$, 10^{-2} T
M01	145	52.0	8.6
M02	105	28.0	4.6
M03	25.0	8.9	2.6
M04	79.5	6.6	1.2
M05	47.0	15.0	2.5
M09	35.0	13.0	1.6
M10	42.5	17.0	1.7
M11	35.0	13.0	1.9
M12	44.0	16.0	1.9
M16	90.0	14.5	2.4
M17	100	22.5	2.2
M18	70.5	18.0	2.0

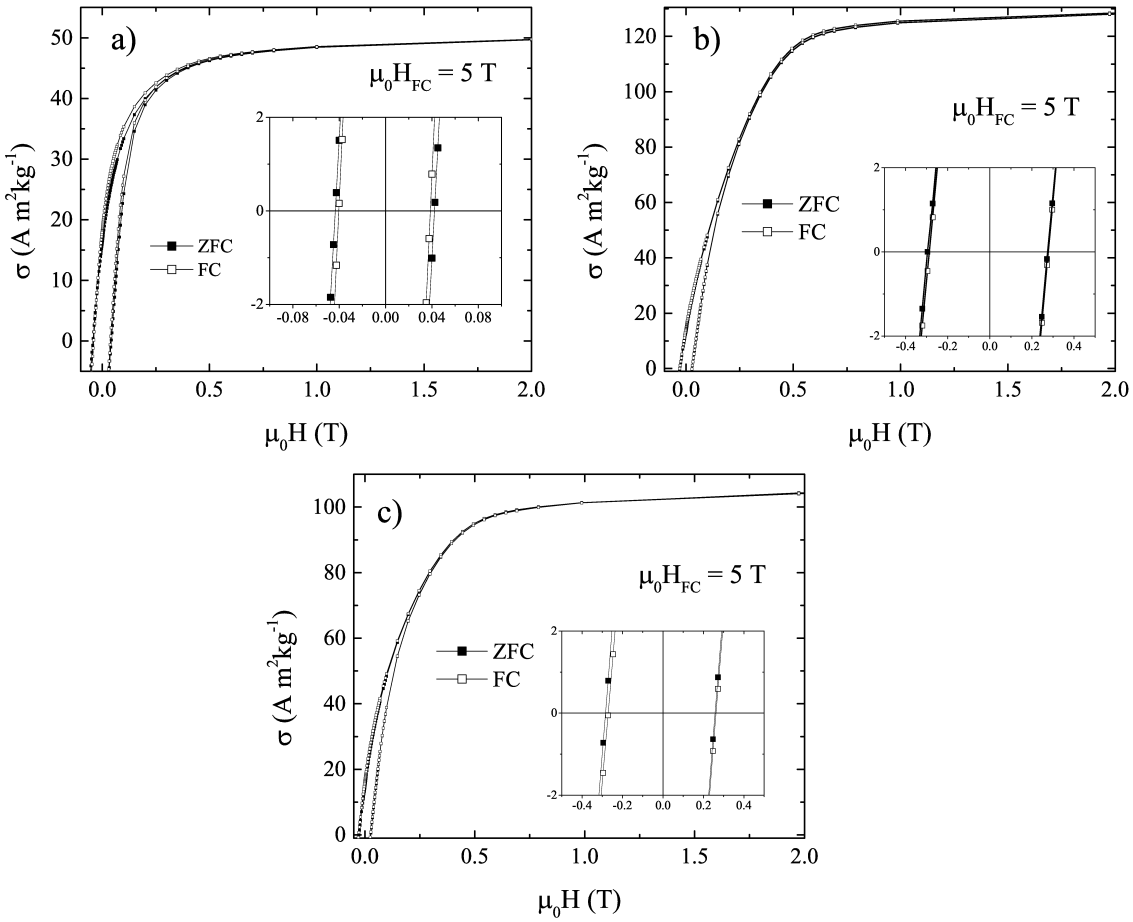

Fig. S3 ZFC and FC (after applying a field $\mu_0 H_{FC}$ = 5 T) magnetization curves at 5 K of samples M13 (a), M15 (b) and M19 (c). Insets show the corresponding low field regions.

APPENDIX A: APPLIED FIELD AND SAMPLE HOLDER CORRECTION IN SQUID MEASUREMENTS

All magnetic measurements obtained with the hybrid SQUID-VSM magnetometer had to be corrected for field errors. The superconducting electromagnet of the instrument can never be completely discharged and, as a consequence, flux is trapped in the magnet at field values above 1000 Oe. The formation of pinning sites leads to errors on the measured field, which consequently is reflected as a virtual increase of the sample's coercive field. This effect can be corrected post-measurement by using a highly stable paramagnetic salt, dysprosium (III) oxide (Dy_2O_3). As a paramagnet, the corresponding magnetization curve at 300K of Dy_2O_3 should consist in an anhysteretic loop showing a linear relationship with the applied field. However, upon measuring the sample, the obtained data shows a quasi-linear response with a coercive field of about 30 Oe. This field error is then corrected by estimating the real value of the field for the Dy_2O_3. The gradient of each of the magnetization curve quadrants is calculated (χ') and the theoretical field value is obtained as the product of the

measured gradient by the measured field ($H_t = \chi' H'$). The field error is expressed as the difference between the measured and theoretical field values divided by the measured gradient:

$$H_{err} = \frac{H' - H_t}{\chi'} \quad \text{(A.1)}$$

The true field is the sum of the error and the measured fields. The obtained correction is valid for any samples measured using the same field steps. An example of the field correction on a Dy_2O_3 standard sample measured at 300 K is shown in Fig. S4.

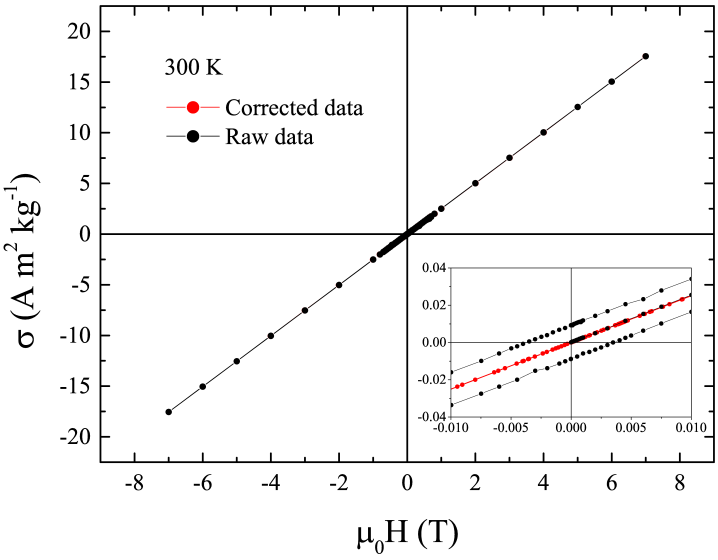

Fig. S4 Magnetization vs field plot of a standard sample of Dy_2O_3 at 300K. Raw and field-corrected data are shown.

APPENDIX B: CHARACTERISTIC LENGTHS CALCULATIONS

The size threshold value from which a multidomain magnetic particle becomes single domain (R_{sd}) can be expressed as a function of the exchange length[33] (l_{ex}) through $R_{sd} = 36\kappa l_{ex}$ (B.1), where $l_{ex} = \left(A / \mu_0 M_S^2\right)^{1/2}$ (B.2), and $\kappa = \left(K / \mu_0 M_S^2\right)^{1/2}$ (B.3), being K the first anisotropy constant at room temperature, κ the dimensionless hardness parameter, μ_0 the permeability of the free space (1.2566×10^{-6} J/A^{2}m) and A the exchange stiffness constant. The latter is given by:

$$A = nJS^2 / a \quad \text{(B.4)}$$

Where n is the number of atoms per unit cell, a the lattice parameter, S the spin momentum and J the exchange constant. J is not directly measurable, but can be in turn estimated from:[53]

$$J \approx 0.3 k_B T_C \quad \text{(B.5)}$$

being T_C the Curie temperature. For $NiFe_2O_4$, T_C = 858 K, and hence $J = 3.55\times10^{-21}$ J. On the other hand, the nickel ferrite structure has 8 Ni, 16 Fe and 32 O atoms in its unit cell; that means n = 56. As only Ni effectively contributes to the net magnetization, n = 8. Substituting J, n and a (8.35×10^{-10} m) in Eq. (B.4), we have $A = 8.50\times10^{-12}$ J/m.

Inserting the corresponding values for $NiFe_2O_4$ (considering $K = 0.7\times10^4$ J/m^3 and $M_S = 2.71\times10^5$ A/m at room temperature) in Eqs. (B.2) and (B.3), it follows that κ= 0.27 and l_{ex} = 9.58 nm, and using these values in Eq. (B.1) we finally obtain R_{SD} = 93.11 nm. Additionally, the theoretical superparamagnetic size limit (R_{SPM}) can be easily calculated from the first anisotropy constant through the expression $R_{SPM} = \left(6k_BT / K\right)^{1/3}$ (B.6). For $NiFe_2O_4$ NPs we obtain R_{SPM} = 15.25 nm.